Stable Sarma state in two-band Fermi systems

Lianyi He and Pengfei Zhuang
Department of Physics, Tsinghua University, Beijing 100084, China
(Received 3 June 2008; published 21 January 2009)

We investigate fermionic superconductivity with mismatched Fermi surfaces in a general two-band system. The exchange interaction between the two bands changes significantly the stability structure of the pairing states. The Sarma state with two gapless Fermi surfaces, which is always unstable in single-band systems, can be the stable ground state in two-band systems. To realize a visible mismatch window for the stable Sarma state, two conditions should be satisfied: a nonzero interband exchange interaction and a large asymmetry between the two bands.

DOI: 10.1103/PhysRevB.79.024511 PACS number(s): 74.20.−z, 03.75.Kk, 05.30.Fk

I. INTRODUCTION

The Cooper pairing with mismatched Fermi surfaces, which has been investigated many years ago,[1,2] promoted new interest in the study of new superconducting materials in strong magnetic field and ultracold fermions due to the realization of superfluidity in resonantly interacting Fermi gases. The well-known theoretical result for *s*-wave weak-coupling superconductors is that, at a critical mismatch, called Chandrasekhar-Clogston limit (CC limit) $h_c=0.707\Delta_0$, where Δ_0 is the zero temperature gap, a first-order phase transition from the gapped BCS state to the normal state occurs.[3] Further theoretical studies showed that the inhomogeneous Fulde-Ferrell-Larkin-Ovchinnikov (FFLO) state[2] may survive in a narrow window between h_c and $h_{\mathrm{FFLO}}=0.754\Delta_0$. However, since the thermodynamic critical field is much smaller than the CC limit due to strong orbit effect,[3] it is hard to observe the CC limit and the FFLO state in ordinary superconductors. In recent years, some experimental evidence for the FFLO state in heavy fermion superconductors,[4] high temperature superconductors[5] and organic superconductors[6] were found. More recently, in the study of ultracold atoms, Fermi superfluidity with population imbalance was realized by MIT and Rice groups independently.[7] The ultracold fermion experiments have promoted a lot of theoretical works[8–11] on the superfluidity mechanism and the phase diagrams for the crossover from Bardeen-Cooper-Schrieffer (BCS) to Bose-Einstein condensation (BEC).[12] The problem of imbalanced pairing is also related to the study of color superconductivity and pion superfluidity in dense quark matter.[13,14]

While most of the theoretical works focus on the inhomogeneous FFLO state, we in this paper are interested in the homogeneous and gapless Sarma state.[1] For weak-coupling superconductors, the Sarma state is located at the maximum of the thermodynamic potential of the system and therefore cannot be the stable ground state. This was called Sarma instability many years ago.[1] The thermodynamic instability of the Sarma state can be traced to the existence of gapless fermion excitations which cause a very large density of state at the gapless Fermi surfaces.[1,2] To realize a stable Sarma state, one should have some mechanism to cure the instability. Forbes *et al.*[15] proposed that, a stable Sarma state is possible in a model with finite range interaction where the momentum dependence of the pairing gap cures the instability. On the other hand, when the attractive interaction becomes strong enough which can be realized in ultracold fermion experiments, the stability of the Sarma state can be changed. While the homogeneous Sarma state is always unstable at the BCS side of the BCS-BEC crossover, it becomes stable in the deep BEC region.[9] However, this stable Sarma state at the BEC side is not the original "interior gap" or "breached pairing" state with two gapless Fermi surfaces proposed by Liu and Wilczek.[16] Since the fermion chemical potential becomes negative in the BEC region, the Sarma state in this case possesses only one gapless Fermi surface, and the matter behaves similar to a Bose-Fermi mixture.[17]

In this paper, we focus on how the multiband structure, which may be realized in solid materials and optical lattices, changes the stability of the Sarma state. We consider a general two-band Fermi system and show that the interband exchange interaction can cure the Sarma instability, and the Sarma state can be the stable ground state in visible parameter regions.

The multiband theory of BCS superconductivity was first introduced by Suhl *et al.*[18] in 1959 to describe the possible multiple band crossings at the Fermi surface. The two-band model has been applied to the study of high-T_c superconductors[19] to effectively describe the particular crystalline and electronic structure. Recently, it is found that the material MgB_2 is a standard two-band superconductor[20] and many experimental data can be explained by the two-band model of BCS superconductivity. Multiband Fermi systems may be realized experimentally with ultracold atoms in optical lattice.[21] For example, if we confine the cold atoms in a one-dimensional periodic external potential, the band structure will form in the confined direction and the matter can be regarded as a multiband system in two dimensions. In this case, by adjusting the coupling strength, one can study the possible BCS-BEC crossover in multiband systems.[19,22] The interband physics in optical lattices is recently studied,[23] and the multigap superfluidity is also possible in nuclear matter.[24]

The paper is organized as follows. In Sec. II we give an introduction to the Sarma state in single-band systems. We discuss the stability of the Sarma state in a general two-band model in Sec. III and summarize in Sec. IV.

II. SARMA STATE IN SINGLE-BAND MODEL

Before discussing the stability of Sarma state in two-band systems, we in this section give a brief introduction to the Sarma state in single-band systems. We start from the following standard BCS-type Hamiltonian:

$$H = \int d^3\mathbf{r}\left[\sum_\sigma \psi_\sigma^\dagger(\mathbf{r})\left(-\frac{\nabla^2}{2m}-\mu_\sigma\right)\psi_\sigma(\mathbf{r}) - U\psi_\uparrow^\dagger(\mathbf{r})\psi_\downarrow^\dagger(\mathbf{r})\psi_\downarrow(\mathbf{r})\psi_\uparrow(\mathbf{r})\right]. \quad (1)$$

We constrain ourselves to discuss systems at zero temperature where the BCS mean-field theory can be applied even at strong coupling.[12] In the mean-field approximation, the Hamiltonian is approximated by

$$H_{\mathrm{mf}} = \int d^3\mathbf{r}\left[\sum_\sigma \psi_\sigma^\dagger(\mathbf{r})\left(-\frac{\nabla^2}{2m}-\mu_\sigma\right)\psi_\sigma(\mathbf{r}) + \Phi(\mathbf{r})\psi_\uparrow^\dagger(\mathbf{r})\psi_\downarrow^\dagger(\mathbf{r}) + \mathrm{H.c.} + \frac{|\Phi(\mathbf{r})|^2}{U}\right], \quad (2)$$

where $\Phi(\mathbf{r})=-U\langle\psi_\downarrow(\mathbf{r})\psi_\uparrow(\mathbf{r})\rangle$ is the order-parameter field of superconductivity. For homogeneous superconductivity, the thermodynamic potential Ω can be obtained by using the standard diagonal method.[18] It can be expressed as

$$\Omega = \frac{\Delta^2}{U} + \int \frac{d^3\mathbf{k}}{(2\pi)^3}\left[(\xi_\mathbf{k}-E_\mathbf{k}) + \sum_\sigma E_\mathbf{k}^\sigma\Theta(-E_\mathbf{k}^\sigma)\right], \quad (3)$$

with the definition of energy dispersions $\xi_\mathbf{k}=\mathbf{k}^2/(2m)-\mu$, $E_\mathbf{k}=\sqrt{\xi_\mathbf{k}^2+\Delta^2}$, $E_\mathbf{k}^\uparrow=E_\mathbf{k}+h$, and $E_\mathbf{k}^\downarrow=E_\mathbf{k}-h$, where $\mu=(\mu_\uparrow+\mu_\downarrow)/2$ and $h=(\mu_\uparrow-\mu_\downarrow)/2$ are, respectively, the averaged and mismatched chemical potentials and Δ is the modulus of $\Phi(\mathbf{r})$.

Without loss of generality, we set $h\geq 0$. The possible ground state of the system corresponds to the stationary point of the thermodynamic potential Ω. This gives the so-called gap equation,

$$\left(\frac{1}{U}-\int\frac{d^3\mathbf{k}}{(2\pi)^3}\frac{\Theta(E_\mathbf{k}^\downarrow)}{2E_\mathbf{k}}\right)\Delta = 0. \quad (4)$$

To properly achieve strong coupling, the chemical potentials should be renormalized by the number equations. The number density n and spin-density imbalance δ can be evaluated as

$$n = n_\uparrow + n_\downarrow = \int\frac{d^3\mathbf{k}}{(2\pi)^3}\left[1-\frac{\xi_\mathbf{k}}{E_\mathbf{k}}\Theta(E_\mathbf{k}^\downarrow)\right],$$

$$\delta = n_\uparrow - n_\downarrow = \int\frac{d^3\mathbf{k}}{(2\pi)^3}\Theta(-E_\mathbf{k}^\downarrow). \quad (5)$$

Whether the Zeeman energy imbalance h or the spin-density imbalance δ is experimentally adjusted depends on detailed systems. For cold atoms, the spin-density imbalance δ is directly tuned, but in superconductors, the Zeeman splitting h is adjusted via an external magnetic field.

A. Stability analysis

If a solution of the gap equation is the ground state of the system, it should be the global minimum of the thermodynamic potential Ω.[15,25] The condition for a local minimum of Ω is that

$$\frac{\partial\Omega(\Delta)}{\partial\Delta}=0, \quad \frac{\partial^2\Omega(\Delta)}{\partial\Delta^2}>0. \quad (6)$$

The first condition corresponds to the gap equation, and the second-order derivative $I=\partial^2\Omega(\Delta)/\partial\Delta^2$ can be evaluated as

$$I = \int\frac{d^3\mathbf{k}}{(2\pi)^3}\frac{\Delta^2}{E_\mathbf{k}^2}\left[\frac{\Theta(E_\mathbf{k}^\downarrow)}{E_\mathbf{k}}-\delta(E_\mathbf{k}^\downarrow)\right]. \quad (7)$$

Let us study the Sarma state with $h>\Delta$ which induces a nonzero-spin-density imbalance δ. At weak coupling, I can be approximately evaluated as

$$\frac{\pi^2 I}{m} \simeq \sqrt{2m\mu}\left[1-\frac{h\Theta(h-\Delta)}{\sqrt{h^2-\Delta^2}}\right], \quad (8)$$

which shows that $\partial^2\Omega(\Delta)/\partial\Delta^2$ is always negative and therefore the Sarma state is unstable.

To achieve the BCS-BEC crossover, we renormalize the coupling constant with the two-body scattering length a_s,

$$\frac{m}{4\pi a_s} = -\frac{1}{U}+\int\frac{d^3\mathbf{k}}{(2\pi)^3}\frac{m}{\mathbf{k}^2}. \quad (9)$$

In this case, we first solve the coupled gap and number equations at fixed total density $n=k_F^3/(3\pi^2)$. The result can be expressed[9] as a function of the dimensionless coupling parameter $g=1/(k_F a_s)$ and the population imbalance $P=\delta/n$. The numerical calculations show that the key quantity I is always negative at the BCS side of the resonance ($a_s<0, g<0$) where the Sarma state has two gapless Fermi surfaces, but the Sarma state can be a stable ground state in the strong-coupling BEC region (roughly for $g>2.2$) where the chemical potential μ become negative. However, this Sarma state has only one gapless Fermi surface and is different from the Fermi-surface topology of the so-called breached pairing state.

B. Solution at weak coupling

At weak coupling where the chemical potential μ is well approximated by the Fermi energy ϵ_F, the gap equation can be approximated by

$$\left[\frac{1}{UN}-\int_0^\Lambda d\xi\frac{\Theta(\sqrt{\xi^2+\Delta^2}-h)}{\sqrt{\xi^2+\Delta^2}}\right]\Delta = 0, \quad (10)$$

where N is the density of state for each spin state at the Fermi surface and Λ is the energy cutoff which plays the role of Debye energy $\hbar\omega_D$ in solids. After the integration and using the condition $\Delta\ll\Lambda$, we find

$$\left[\frac{1}{UN}-\ln\frac{2\Lambda}{\Delta}+\Theta(h-\Delta)\ln\frac{h+\sqrt{h^2-\Delta^2}}{\Delta}\right]\Delta = 0. \quad (11)$$

There are three possible solutions to the gap Eq. (11) for $h\neq 0$. The first is the trivial normal phase with $\Delta_N=0$. The

second corresponds to the ordinary fully gapped BCS solution satisfying $\Delta > h$,

$$\Delta_{\mathrm{BCS}} = \Delta_0 = 2\Lambda e^{-1/(UN)}. \tag{12}$$

The third solution, i.e., the gapless Sarma state satisfying $\Delta < h$, can be analytically evaluated via the comparing with the BCS solution. It is[26]

$$\Delta_S = \sqrt{\Delta_0(2h - \Delta_0)}. \tag{13}$$

Using the weak-coupling approximation, the grand potential Ω for various solutions can be expressed as

$$\Omega = \frac{\Delta^2}{U} + 2N\int_0^{\Lambda} d\xi[\xi - \sqrt{\xi^2 + \Delta^2} + (\sqrt{\xi^2 + \Delta^2} - h)\Theta(h - \sqrt{\xi^2 + \Delta^2})]. \tag{14}$$

Performing the integral over ξ and using the condition $\Delta \ll \Lambda$ as well as the gap equation to cancel the cut-off dependence, we have

$$\Omega = -\frac{N}{2}\Delta^2 - \Theta(h - \Delta)Nh\sqrt{h^2 - \Delta^2}. \tag{15}$$

Note that we have set the grand potential of the normal state at $h=0$ to be zero, $\Omega_N(h=0)=0$. To see why the Sarma state is always thermodynamically unstable, one should calculate the grand potential differences between Sarma and other two states,[26]

$$\Omega_S - \Omega_{\mathrm{BCS}} = N(\Delta_0 - h)^2,$$

$$\Omega_S - \Omega_N = \frac{N}{2}(\Delta_0 - 2h)^2, \tag{16}$$

which confirm that the Sarma state always has higher potential than the BCS and normal states. As a consequence, there exists a first-order phase transition from BCS to normal state. From the result

$$\Omega_{\mathrm{BCS}} - \Omega_N = \frac{N}{2}(2h^2 - \Delta_0^2), \tag{17}$$

the transition occurs at the CC limit of BCS superconductivity, $h_c = \Delta_0/\sqrt{2}$.

III. SARMA STATE IN TWO-BAND MODEL

We in this section turn to the two-band model. Since the goal of this paper is to search for the possibility of stable Sarma state in general two-band Fermi systems, we consider a continuum Hamiltonian and neglect the details of the band structure in different systems. We will show that the key point is the interband scattering which can make the Sarma state stable in multiband systems. The possible complicated lattice structure in various materials and optical lattices will not qualitatively change our conclusion. The obtained conclusion is generic and may be useful for the study of superconducting materials and ultracold atom gases.

The continuum Hamiltonian of the two-band model can be written as[18]

$$H = \int d^3\mathbf{r}\left[\sum_{\nu,\sigma}\psi^{\dagger}_{\nu\sigma}(\mathbf{r})\left(-\frac{\nabla^2}{2m_\nu} - \mu_{\nu\sigma}\right)\psi_{\nu\sigma}(\mathbf{r}) - \sum_{\nu,\lambda} U_{\nu\lambda}\psi^{\dagger}_{\nu\uparrow}(\mathbf{r})\psi^{\dagger}_{\nu\downarrow}(\mathbf{r})\psi_{\lambda\downarrow}(\mathbf{r})\psi_{\lambda\uparrow}(\mathbf{r})\right], \tag{18}$$

where $\nu,\lambda = 1,2$ denote the band and $\sigma = \uparrow,\downarrow$ denotes the direction of fermion spin. In superconductors, the band degrees of freedom usually come from the particular crystalline and electronic structure of the materials. In ultracold atom gases, these degrees of freedom may come from different hyperfine states or different atom species or the external periodic lattice potential. In general case, the effective fermion mass depends only on the band index, but the chemical potential is related to both the band and spin indices due to the existence of external magnetic field or population imbalance. The constants $U_{11} \equiv U_1$ and $U_{22} \equiv U_2$ are the intraband couplings, and $U_{12} = U_{21} \equiv J$ is the interband exchange coupling. For vanishing J, the model is reduced to a simple system with two independent bands. In the following we focus on how the interband coupling J changes the stability of the Sarma state.

First we calculate the thermodynamic potential of the two-band Hamiltonian. In the mean-field approximation, the Hamiltonian is approximated by

$$H_{\mathrm{mf}} = \int d^3\mathbf{r}\left\{\sum_{\nu,\sigma}\psi^{\dagger}_{\nu\sigma}(\mathbf{r})\left(-\frac{\nabla^2}{2m_\nu} - \mu_{\nu\sigma}\right)\psi_{\nu\sigma}(\mathbf{r}) + \sum_{\nu}[\Phi_\nu(\mathbf{r})\psi^{\dagger}_{\nu\uparrow}(\mathbf{r})\psi^{\dagger}_{\nu\downarrow}(\mathbf{r}) + \mathrm{H.c.}] + \frac{1}{G}\{U_2|\Phi_1(\mathbf{r})|^2 + U_1|\Phi_2(\mathbf{r})|^2 - J[\Phi_1^*(\mathbf{r})\Phi_2(\mathbf{r}) + \Phi_2^*(\mathbf{r})\Phi_1(\mathbf{r})]\}\right\}, \tag{19}$$

where $\Phi_\nu(\mathbf{r}) = -\Sigma_\lambda U_{\nu\lambda}\langle\psi_{\lambda\downarrow}(\mathbf{r})\psi_{\lambda\uparrow}(\mathbf{r})\rangle$ are two order-parameter fields of the superconductivity and G is defined as $G = U_1U_2 - J^2$. For homogeneous superconductivity, the thermodynamic potential Ω of this two-band model can be obtained by using the standard diagonal method.[18] It can be expressed as

$$\Omega = \frac{1}{G}[U_2\Delta_1^2 + U_1\Delta_2^2 - 2J\Delta_1\Delta_2\cos(\varphi_1 - \varphi_2)] + \sum_{\nu}\int\frac{d^3\mathbf{k}}{(2\pi)^3}\left[(\xi_{\mathbf{k}\nu} - E_{\mathbf{k}\nu}) + \sum_{\sigma}E^{\sigma}_{\mathbf{k}\nu}\Theta(-E^{\sigma}_{\mathbf{k}\nu})\right], \tag{20}$$

with the definition of energy dispersions $\xi_{\mathbf{k}\nu} = \mathbf{k}^2/(2m_\nu) - \mu_\nu$, $E_{\mathbf{k}\nu} = \sqrt{\xi^2_{\mathbf{k}\nu} + \Delta^2_\nu}$, $E^{\uparrow}_{\mathbf{k}\nu} = E_{\mathbf{k}\nu} + h_\nu$, and $E^{\downarrow}_{\mathbf{k}\nu} = E_{\mathbf{k}\nu} - h_\nu$, where $\mu_\nu = (\mu_{\nu\uparrow} + \mu_{\nu\downarrow})/2$ and $h_\nu = (\mu_{\nu\uparrow} - \mu_{\nu\downarrow})/2$ are, respectively, the averaged and mismatched chemical potentials, and Δ_ν is the modulus of Φ_ν and φ_ν is their phases through the definition $\Phi_\nu = \Delta_\nu e^{i\varphi_\nu}$. Without loss of generality, we take $h_\nu > 0$. For $J > 0$, the choice of $\varphi_1 = \varphi_2$ is favored, otherwise there is $\varphi_1 = \varphi_2 + \pi$. We assume $J > 0$ and set $\varphi_1 = \varphi_2$.

The possible ground state of the system corresponds to the stationary point of the thermodynamic potential Ω. This gives the so-called gap equations,

$$\left(\frac{U_{\bar{\nu}\bar{\nu}}}{G}-\int\frac{d^3\mathbf{k}}{(2\pi)^3}\frac{\Theta(E^{\downarrow}_{\mathbf{k}\nu})}{2E_{\mathbf{k}\nu}}\right)\Delta_\nu-\frac{J}{G}\Delta_{\bar{\nu}}=0, \tag{21}$$

with $\bar{\nu}=1$ for $\nu=2$ and $\bar{\nu}=2$ for $\nu=1$. The gap equations are essentially the same as derived in Ref. 18. To properly achieve strong coupling, the chemical potentials should be renormalized by the number equations. The number equations for the fermion density n_ν and density imbalance δ_ν for the νth band can be evaluated as

$$n_\nu=n_{\nu\uparrow}+n_{\nu\downarrow}=\int\frac{d^3\mathbf{k}}{(2\pi)^3}\left[1-\frac{\xi_{\mathbf{k}\nu}}{E_{\mathbf{k}\nu}}\Theta(E^{\downarrow}_{\mathbf{k}\nu})\right],$$

$$\delta_\nu=n_{\nu\uparrow}-n_{\nu\downarrow}=\int\frac{d^3\mathbf{k}}{(2\pi)^3}\Theta(-E^{\downarrow}_{\mathbf{k}\nu}), \tag{22}$$

and the total density n and total density imbalance δ of the system are defined as $n=n_1+n_2$ and $\delta=\delta_1+\delta_2$, respectively.

A. Stability analysis

Let us now discuss qualitatively what happens when the mismatch h_ν increases. For vanishing mismatch, the system is in a fully gapped BCS state with $\Delta_1\equiv\Delta_{10}$ and $\Delta_2\equiv\Delta_{20}$, and the spin-density imbalance δ is zero. With increasing h_ν, while the BCS state is still a solution of the gap equations, there may appear another solution (Sarma) where at least one of the pairing gap Δ_ν is less than the corresponding mismatch, namely, $h_\nu>\Delta_\nu$. In this state, the dispersion of the quasiparticle $E^{\downarrow}_{\mathbf{k}\nu}$ becomes gapless and the system has a nonzero spin-density imbalance δ. Note that the normal state with vanishing condensate is always a solution of the gap equations and becomes the ground state when both h_1 and h_2 are large enough.

Different from the conventional Sarma state in single-band models, we may have two types of Sarma states in two-band systems. The first type (type I) is the solution where both mismatches are larger than the corresponding pairing gaps, namely, $h_1>\Delta_1$ and $h_2>\Delta_2$. For this type, there exist gapless excitations in both bands. The second type (type II) is the solution where only one mismatch is larger than the corresponding pairing gap, $h_1>\Delta_1$ and $h_2<\Delta_2$ or $h_1<\Delta_1$ and $h_2>\Delta_2$. For this type, gapless excitations exist only in one band. We will show in the following that the stabilities of these two types of Sarma states are quite different.

A numerical example which supports the above argument is shown in Fig. 1 for two symmetric bands with $U_1=U_2$. For the sake of simplicity, in our numerical examples presented here, we assume the same effective masses, chemical potentials, and mismatches for the two bands, i.e., $m_1=m_2\equiv m$, $\mu_1=\mu_2\equiv\mu$, and $h_1=h_2\equiv h$, this means that only the total density n and total spin-density imbalance δ can be adjusted. We write U_1 and U_2 in terms of the s-wave scattering length a_ν with a momentum cutoff k_0, $U_\nu^{-1}=-m/(4\pi a_\nu)+\int_{|\mathbf{k}|<k_0}d^3\mathbf{k}/(2\pi)^3m/\mathbf{k}^2$. Our qualitative conclusions do not depend on the used regularization scheme. In the case of $U_1=U_2$, the solutions of the gap equations are distributed symmetrically in the $\Delta_1-\Delta_2$ plane. Besides the familiar BCS and normal states which are, respectively, the global minimum and a local minimum in Fig. 1, we have some Sarma states in the potential contour. The Sarma states C and D are of type I, C is the global maximum and D indicates two saddle points. The type II Sarma states are marked by A and B, corresponding, respectively, to two local minima and two saddle points.

If a solution of the gap equations is the ground state of the system, it should be the global minimum of the thermodynamic potential Ω.[15,25] The condition for a local minimum of Ω is that the matrix

$$\mathcal{M}=\begin{pmatrix}\dfrac{\partial^2\Omega(\Delta_1,\Delta_2)}{\partial\Delta_1^2} & \dfrac{\partial^2\Omega(\Delta_1,\Delta_2)}{\partial\Delta_1\,\partial\Delta_2}\\ \dfrac{\partial^2\Omega(\Delta_1,\Delta_2)}{\partial\Delta_2\,\partial\Delta_1} & \dfrac{\partial^2\Omega(\Delta_1,\Delta_2)}{\partial\Delta_2^2}\end{pmatrix} \tag{23}$$

should have only positive eigenvalues, namely, $\det\mathcal{M}>0$ and $\mathrm{Tr}\,\mathcal{M}>0$. The second-order derivatives can be evaluated as

$$\frac{\partial^2\Omega(\Delta_1,\Delta_2)}{\partial\Delta_\nu^2}=\frac{2J}{G}\frac{\Delta_{\bar{\nu}}}{\Delta_\nu}+I_\nu,$$

$$\frac{\partial^2\Omega(\Delta_1,\Delta_2)}{\partial\Delta_\nu\,\partial\Delta_{\bar{\nu}}}=-\frac{2J}{G}, \tag{24}$$

with the quantities I_ν defined as

$$I_\nu=\int\frac{d^3\mathbf{k}}{(2\pi)^3}\frac{\Delta_\nu^2}{E^2_{\mathbf{k}\nu}}\left[\frac{\Theta(E^{\downarrow}_{\mathbf{k}\nu})}{E_{\mathbf{k}\nu}}-\delta(E^{\downarrow}_{\mathbf{k}\nu})\right]. \tag{25}$$

For vanishing interband coupling $J=0$, the stability condition becomes

$$I_1I_2>0,\quad I_1+I_2>0. \tag{26}$$

Note that the properties of the functions I_1 and I_2 are the same as the function I defined in Sec. II. Thus at the BCS side, namely, for $a_1<0$ and $a_2<0$, the Sarma state is unstable.

Now we discuss how the interband coupling J modifies the Sarma instability at the BCS side. For $J\neq0$, the stability condition reads

$$\frac{2J}{G}\left(\frac{\Delta_1}{\Delta_2}I_1+\frac{\Delta_2}{\Delta_1}I_2\right)+I_1I_2>0,$$

$$\frac{2J}{G}\left(\frac{\Delta_1}{\Delta_2}+\frac{\Delta_2}{\Delta_1}\right)+I_1+I_2>0. \tag{27}$$

For the type I Sarma state with $h_1>\Delta_1$ and $h_2>\Delta_2$, we have $I_1<0$ and $I_2<0$. In this case, we can exactly prove that the above two inequalities cannot be satisfied simultaneously. This type of Sarma state should correspond to the maximum or saddle point of the thermodynamic potential and is hence unstable, such as points C and D in Fig. 1. However, the situation changes for the type II Sarma state. Without loss of

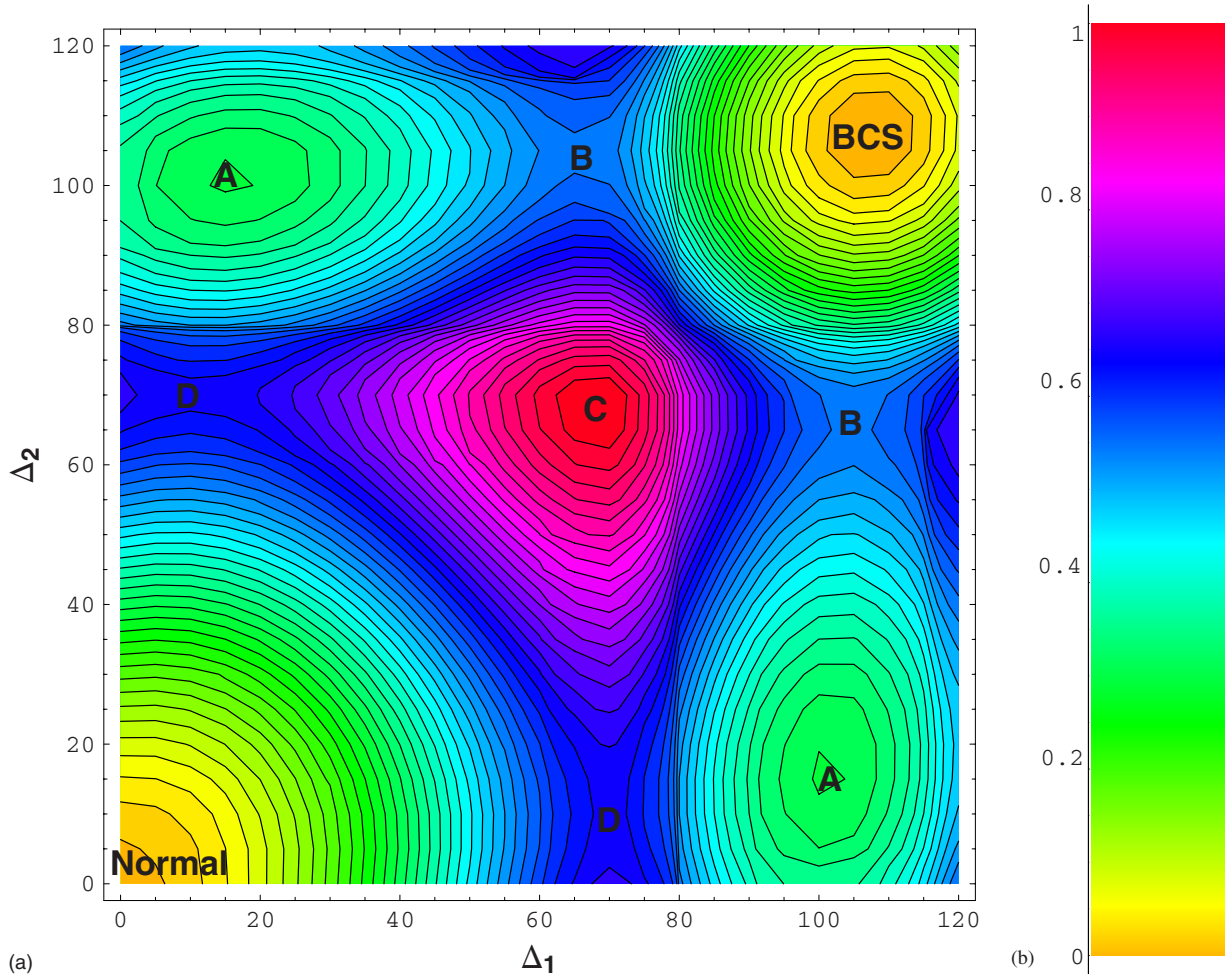

FIG. 1. (Color online) The thermodynamic potential contour $\Omega(\Delta_1,\Delta_2)$ for two symmetric bands with $U_1=U_2$. A proper unit is chosen such that the Fermi energy $\epsilon_F=200$. The values of the other parameters are $k_0=100k_F$, $J=10^{-4}U_0$, with $U_0=4\pi/(mk_F)$, $(k_Fa_1)^{-1}=(k_Fa_2)^{-1}=-0.5$, and $h=75$, where $k_F\simeq\sqrt{2m\mu}$ is the Fermi momentum. The band on the right shows the relative strength of Ω corresponding to different colors. For the parameter setting, we have $U_1=U_2\simeq 0.0156U_0$, and hence $J\ll U_1,U_2$.

generality, let us discuss the case with $h_1>\Delta_1$ and $h_2<\Delta_2$. In this case, only the first band is gapless, and hence $I_1<0$ and $I_2>0$. From $I_2>0$, the above two inequalities are equivalent to the following one:

$$\frac{2J}{G}\frac{\Delta_2}{\Delta_1}+I_1\left(1+\frac{2J}{GI_2}\frac{\Delta_1}{\Delta_2}\right)>0. \tag{28}$$

Even though $I_1<0$, this condition can be satisfied provided that a nonzero interband coupling J is turned on. Suppose the solution of the gap equations satisfies $\Delta_1\ll\Delta_2$ and Δ_1 is not quite close to h_1, which corresponds to the case with large polarization δ_1, the first term in Eq. (28) is large but the modulus of the second term is relatively small, and therefore the stability condition can be satisfied, such as point A at the upper-left corner in Fig. 1. However, on the other hand, for $\Delta_1\lesssim h_1$ which corresponds to the case with small polarization $\delta_1\to 0$, the absolute value of I_1 is very large, and the Sarma state maybe unstable, which corresponds to the saddle point B in the upper part of Fig. 1.

We conclude that, in two-band Fermi systems with nonzero interband pairing interaction, the Sarma state can become at least the local minimum of the thermodynamic potential and therefore should be a potential candidate of the ground state.

However, the condition $J\neq 0$ is not sufficient for us to have a real stable Sarma state. For the case with two symmetric bands shown in Fig. 1, we found that the global minimum is always the BCS or normal state for any mismatch h, which means that the Sarma state cannot be the ground state even though it can be a local minimum. However, this can be significantly changed if some asymmetry between the two bands, such as unequal couplings $U_1\neq U_2$, is turned on. In Figs. 2 and 3, we show the potential contour with $U_1\neq U_2$ for three values of h. In this case, the number of Sarma solutions is largely suppressed due to the asymmetry, especially the state C in Fig. 1 as the global maximum of Ω disappears. Without regard to the saddle points which are impossible to be stable solutions, the only Sarma state marked in Figs. 2 and 3 appears to be the global minimum of the system when the mismatch h is in a suitable region. From the top to the bottom in Figs. 2 and 3, when the mismatch h increases, the global minimum changes from the BCS state to the Sarma state and then to the normal state. In contrast to

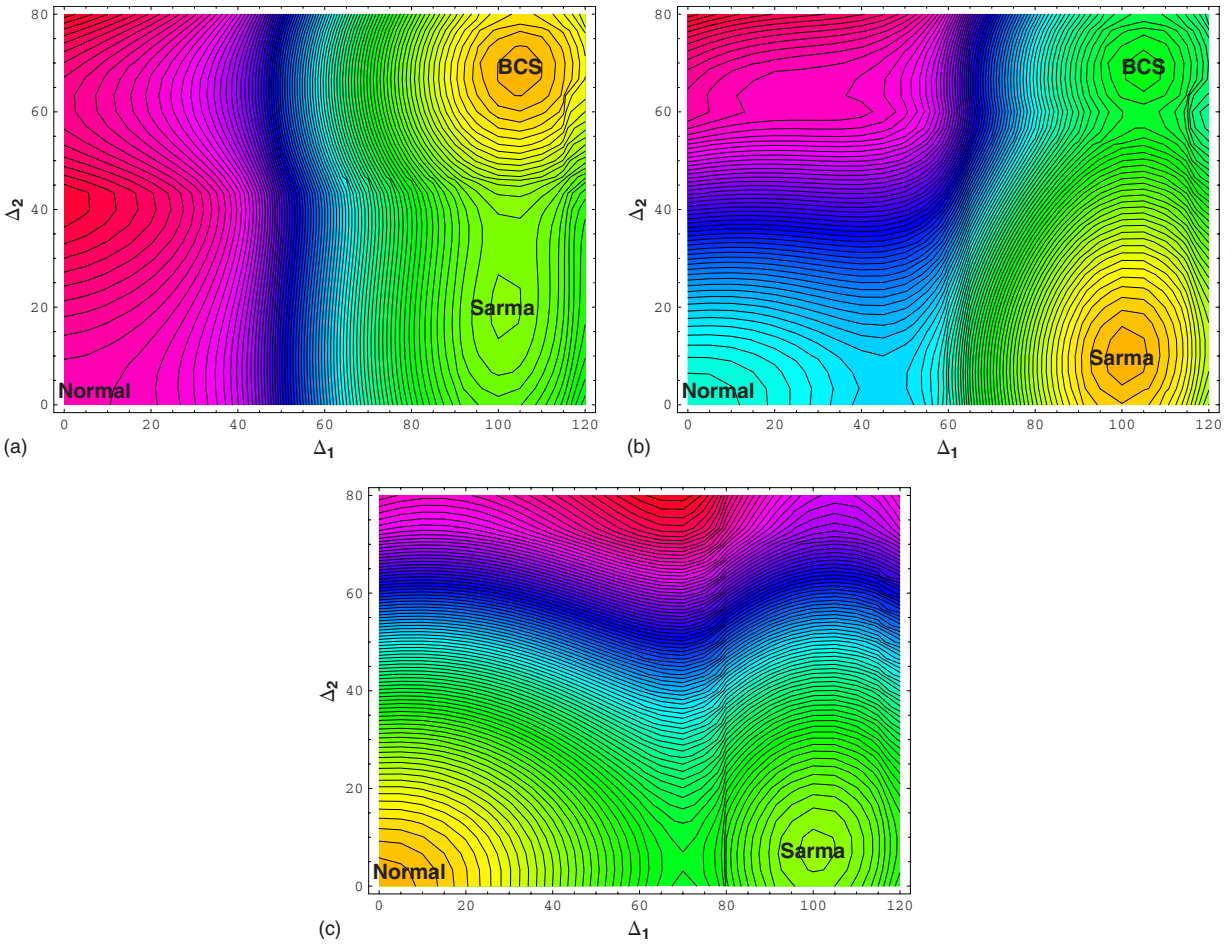

FIG. 2. (Color online) The thermodynamic potential contour $\Omega(\Delta_1,\Delta_2)$ for two different bands with $(k_Fa_1)^{-1}=-0.5$ and $(k_Fa_2)^{-1}=-0.8$ at $h=45$ (a), 60 (b), and 75 (c). The other parameters are the same as that in Fig. 1.

the conventional single-band model where only one first-order phase transition from the BCS to normal state is predicted, we have in this two-band system two first-order phase transitions when h increases: The first is from the BCS to Sarma state and the second is from the Sarma to normal state. The first-order phase transition from BCS to Sarma state was found in Ref. 15 by considering the momentum structure of the pairing gap. For ultracold atom gases, the chemical potential mismatch h should be replaced by the spin population imbalance δ. However, the phase structure should be essentially independent of the assembles one used,[15,25] we here do not consider the case with fixed δ.

Let us compare the numerical results presented in Figs. 2 and 3. In Fig. 3, the coupling asymmetry is much larger than that in Fig. 2, we have $\Delta_{10}/\Delta_{20}\simeq 1.5$ in Fig. 2 and $\Delta_{10}/\Delta_{20}\simeq 4$ in Fig. 3. We find that the h window for the Sarma state is wider when the coupling asymmetry becomes larger. In Fig. 2, the window for Sarma state is roughly from $h=52$ to $h=71$, and the CC limit is about $h_c\simeq\Delta_{20}$. In Fig. 3, this window is roughly from $h=20$ to $h=70$, and the CC limit is about $h_c\simeq 2.7\Delta_{20}$.

B. Solutions at weak coupling

At weak coupling, the same tricks used in Sec. II can be employed. For convenience, we define here a function,

$$F(\Delta,h)=\int_0^\Lambda d\xi\frac{\Theta(\sqrt{\xi^2+\Delta^2}-h)}{\sqrt{\xi^2+\Delta^2}}$$
$$\simeq \ln\frac{2\Lambda}{\Delta}-\Theta(h-\Delta)\ln\frac{h+\sqrt{h^2-\Delta^2}}{\Delta}, \quad (29)$$

and express the gap equations of our two-band model in terms of it,

$$\left[\frac{U_2}{GN_1}-F(\Delta_1,h_1)\right]\Delta_1-\frac{J}{GN_1}\Delta_2=0,$$
$$\left[\frac{U_1}{GN_2}-F(\Delta_2,h_2)\right]\Delta_2-\frac{J}{GN_2}\Delta_1=0, \quad (30)$$

where N_1 and N_2 are the densities of state at the Fermi surfaces for the two bands. Unlike the single-band model, the above coupled gap equations cannot be solved analytically. With the numerical solutions Δ_1 and Δ_2, the thermodynamic potential can be evaluated as

$$\Omega=-\sum_\nu\left[\frac{N_\nu}{2}\Delta_\nu^2+\Theta(h_\nu-\Delta_\nu)N_\nu h_\nu\sqrt{h_\nu^2-\Delta_\nu^2}\right]. \quad (31)$$

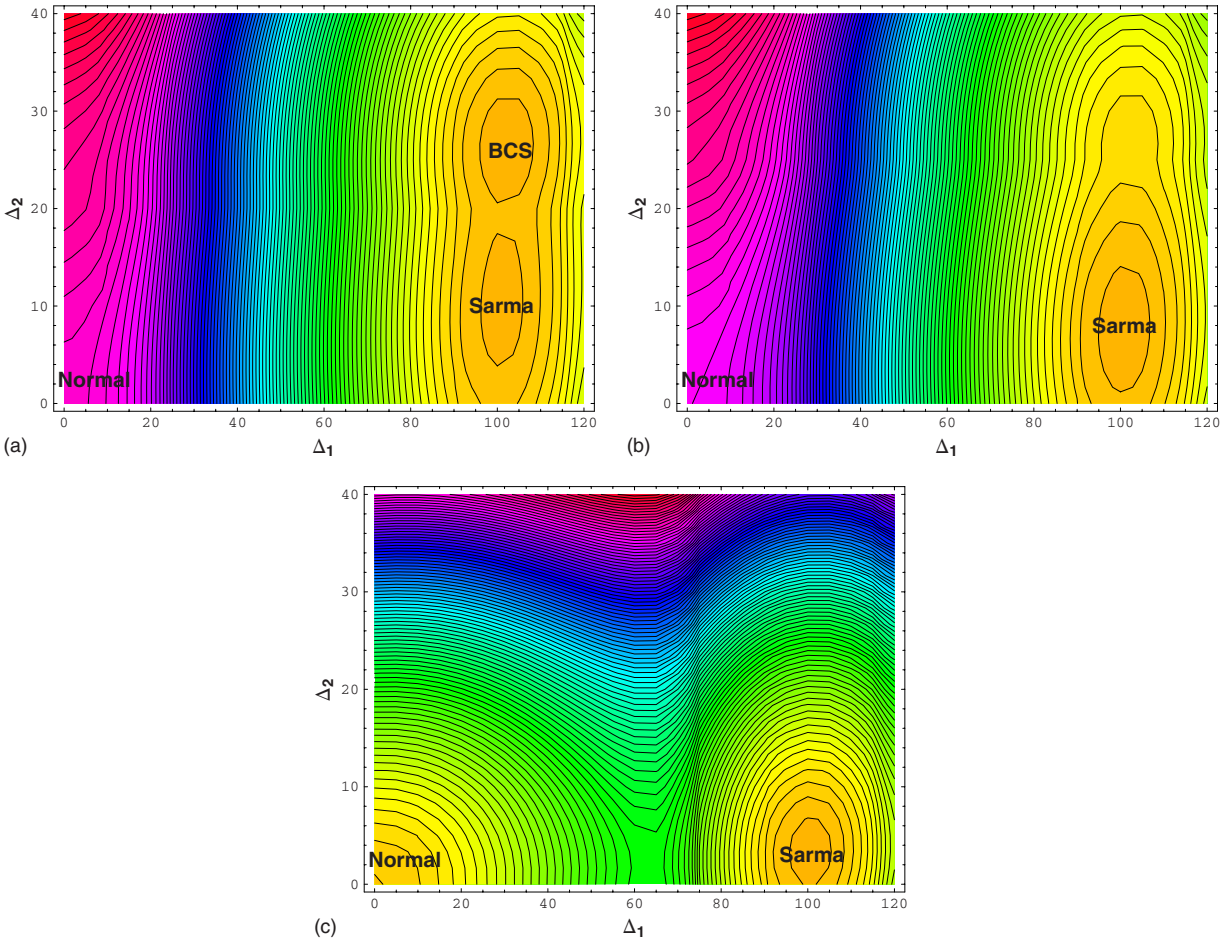

FIG. 3. (Color online) The thermodynamic potential contour $\Omega(\Delta_1,\Delta_2)$ for two different bands with $(k_F a_1)^{-1}=-0.5$ and $(k_F a_2)^{-1}=-1.5$ at $h=20$ (a), 25 (b), and 70 (c). The other parameters are the same as that in Fig. 1.

For the sake of simplicity, we consider the case $h_1=h_2=h$ which corresponds to the realistic two-band superconductors in strong magnetic field. Let us assume $U_1N_1>U_2N_2$ which leads to $\Delta_1>\Delta_2$. According to the stability analysis, we have three possible ground states: (1) the normal state with $\Delta_1=\Delta_2=0$; (2) the gapped BCS state with energy gaps $\Delta_1\equiv\Delta_{10}>h$ and $\Delta_2\equiv\Delta_{20}>h$; and (3) the gapless Sarma state where only $\Delta_1>h$ but $\Delta_2<h$. We focus here on the case with $\Delta_2\ll\Delta_1$ and $J\ll\sqrt{U_1U_2}$. In this case, the solution of Δ_1 is approximately independent of h and is given by

$$\Delta_1=\Delta_{10}\simeq 2\Lambda e^{-1/(U_1N_1)}, \tag{32}$$

and the Sarma solution for Δ_2 is determined by the following equation:

$$\ln\frac{\Delta_{20}}{h+\sqrt{h^2-\Delta_2^2}}=\frac{J\Delta_{10}}{U_1U_2N_2}\left(\frac{1}{\Delta_{20}}-\frac{1}{\Delta_2}\right), \tag{33}$$

where Δ_{20} is obtained by the equation

$$\frac{1}{U_2N_2}-\ln\frac{2\Lambda}{\Delta_{20}}=\frac{J}{U_1U_2N_2}\frac{\Delta_{10}}{\Delta_{20}}. \tag{34}$$

We have numerically checked that the above approximation is sufficiently good for the scaled solution $y=\Delta_2/\Delta_{20}$ as a function of $x=h/\Delta_{20}$. Note that for $J=0$ the conventional Sarma solution $y=\sqrt{2x-1}(0.5<x<1)$ is recovered, but for $J\neq 0$ the Sarma solution is qualitatively changed: $y=0$ cannot be a solution and there exist solutions for $x>1$. The solutions for both cases of $J=0$ and $J\neq 0$ are illustrated in Fig. 4. We find that for $J\neq 0$ the Sarma solution is quite different from the conventional result. Unlike the well-known Sarma solution which exists in the region $0.5<x<1$, for $J\neq 0$ the Sarma state exists almost in the region $x>1$ where the BCS solution $y=1$ disappears. Obviously, in a narrow region $x\lesssim 1$ there exists a branch of the conventional type which is unstable, and the multivalue behavior of y means a first-order BCS-Sarma phase transition at a critical field x_1 which is slightly smaller than 1.

To discuss the thermodynamic stability of the Sarma state, we then need to compare it with the normal state. In the case of $\Delta_2<h$, we find

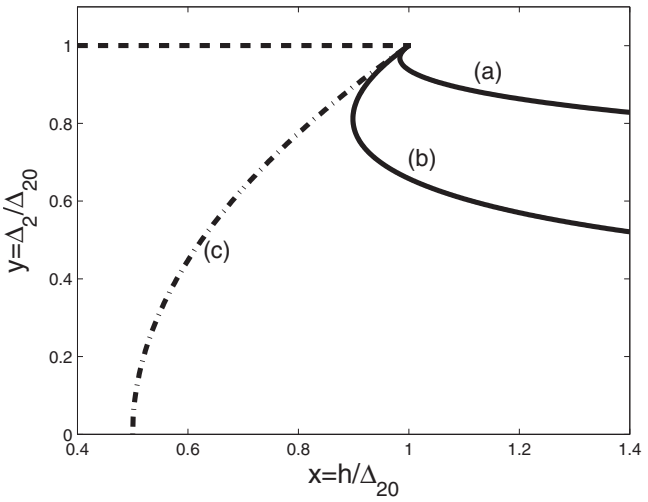

FIG. 4. The solution $y=\Delta_2/\Delta_{20}$ to the gap equations as a function of $x=h/\Delta_{20}$. The dashed line denotes the BCS solution $y=1$ in the region $0<x<1$. The solid lines (a) and (b) are the Sarma solutions for $J\neq 0$. In the calculations, we take $N_1/N_2=1.5$ and $J/\sqrt{U_1U_2}=0.07$. For (a) we take $(U_1N_1)/(U_2N_2)=3$ which leads to $\Delta_{10}/\Delta_{20}\simeq 9$, and for (b) we have $(U_1N_1)/(U_2N_2)=1.67$ and hence $\Delta_{10}/\Delta_{20}\simeq 3$. The dot-dashed line (c) is the conventional Sarma solution for $J=0$, $y=\sqrt{2x-1}$ in the region $0.5<x<1$.

$$\Omega_S-\Omega_N=\frac{N_1}{2}(2h^2-\Delta_1^2)+\frac{N_2}{2}(2h^2-\Delta_2^2-2h\sqrt{h^2-\Delta_2^2}). \tag{35}$$

Some analytical estimations can be made. For large asymmetry $\Delta_2\ll\Delta_1$, around the h-window $h\sim\Delta_{20}$ but $h\ll\Delta_{10}$ for the Sarma state, the sign of the quantity $\Omega_S-\Omega_N$ is dominated by the first term if N_1 is not much smaller than N_2. In this case, the BCS solution is absent and the Sarma state is the stable ground state. This argument confirms our conclusion from the numerical results in Figs. 2 and 3: the h window for stable Sarma state is wider when the asymmetry between the two bands becomes larger. This means that the CC limit of such a two-band superconductor can be much higher than the conventional value $h_c=0.707\Delta_{20}$.

IV. SUMMARY

We have studied the stability of Sarma state in two-band Fermi systems via both the stability analysis and analytical solution at weak coupling. From the stability analysis, the Sarma state can be the minimum of the thermodynamic potential and hence a possible candidate of the ground state if the interband exchange interaction is turned on. Both numerical and analytical studies show that a large asymmetry between the two bands or the two pairing gaps is an important condition for thermodynamic stability of the Sarma state. When the condition is satisfied, two first-order phase transitions will occur when the mismatch increases; one is from the BCS to Sarma state at a lower mismatch and the other is from the Sarma to normal state at a higher mismatch. Our predictions could be tested in multiband superconductors and ultracold atom gases, and such a gapless superconductor may have many unusual properties, such as magnetism and large spin susceptibility.[27,28]

ACKNOWLEDGMENTS

We thank W. V. Liu and M. Iskin for useful communications and Y. Liu and X. Hao for help in numerical calculations. This work was supported by the NSFC Grants No. 10575058 and No. 10735040 and the National Research Program Grant No. 2006CB921404.

[1] G. Sarma, J. Phys. Chem. Solids **24**, 1029 (1963).
[2] P. Fulde and R. A. Ferrell, Phys. Rev. **135**, A550 (1964); A. I. Larkin and Yu. N. Ovchinnikov, Sov. Phys. JETP **20**, 762 (1965).
[3] B. S. Chandrasekhar, Appl. Phys. Lett. **1**, 7 (1962); A. M. Clogston, Phys. Rev. Lett. **9**, 266 (1962).
[4] K. Gloos, R. Modler, H. Schimanski, C. D. Bredl, C. Geibel, F. Steglich, A. I. Buzdin, N. Sato, and T. Komatsubara, Phys. Rev. Lett. **70**, 501 (1993); R. Modler, P. Gegenwart, M. Lang, M. Deppe, M. Weiden, T. Luhmann, C. Geibel, F. Steglich, C. Paulsen, J. L. Tholence, N. Sato, T. Komatsubara, Y. Onuki, M. Tachiki, and S. Takahashi, *ibid.* **76**, 1292 (1996); A. Bianchi, R. Movshovich, C. Capan, P. G. Pagliuso, and J. L. Sarrao, *ibid.* **91**, 187004 (2003).
[5] J. L. O'Brien, H. Nakagawa, A. S. Dzurak, R. G. Clark, B. E. Kane, N. E. Lumpkin, N. Miura, E. E. Mitchell, J. D. Goettee, J. S. Brooks, D. G. Rickel, and R. P. Starrett, Phys. Rev. B **61**, 1584 (2000).
[6] L. Balicas, J. S. Brooks, K. Storr, S. Uji, M. Tokumoto, H. Tanaka, H. Kobayashi, A. Kobayashi, V. Barzykin, and L. P. Gor'kov, Phys. Rev. Lett. **87**, 067002 (2001); M. A. Tanatar, T. Ishiguro, H. Tanaka, and H. Kobayashi, Phys. Rev. B **66**, 134503 (2002).
[7] M. W. Zwierlein, A. Schirotzek, C. H. Schunck, and W. Ketterle, Science **311**, 492 (2006); G. B. Partridge, W. Li, R. I. Kamar, Y.-an Liao, and R. G. Hulet, *ibid.* **311**, 503 (2006).
[8] P. F. Bedaque, H. Caldas, and G. Rupak, Phys. Rev. Lett. **91**, 247002 (2003); A. Sedrakian, J. Mur-Petit, A. Polls, and H. Müther, Phys. Rev. A **72**, 013613 (2005); L. He, M. Jin, and P. Zhuang, Phys. Rev. B **73**, 214527 (2006); **74**, 214516 (2006).
[9] C. H. Pao, S.-T. Wu, and S.-K. Yip, Phys. Rev. B **73**, 132506 (2006); D. E. Sheehy and L. Radzihovsky, Phys. Rev. Lett. **96**, 060401 (2006); D. T. Son and M. A. Stephanov, Phys. Rev. A **74**, 013614 (2006); H. Hu and X. J. Liu, *ibid.* **73**, 051603(R) (2006); M. Mannarelli, G. Nardulli and M. Ruggieri, *ibid.* **74**, 033606 (2006); A. Bulgac and M. McNeil Forbes, *ibid.* **75**, 031605(R) (2007).
[10] J. Kinnunen, L. M. Jensen, and P. Törmä, Phys. Rev. Lett. **96**, 110403 (2006); P. Pieri and G. C. Strinati, *ibid.* **96**, 150404 (2006); T. N. De Silva and E. J. Mueller, *ibid.* **97**, 070402

(2006); K. Machida, T. Mizushima, and M. Ichioka, *ibid.* **97**, 120407 (2006).
[11] D. E. Sheehy and L. Radzihovsky, Ann. Phys. (N.Y.) **322**, 1790 (2007).
[12] A. J. Leggett, *Modern Trends in the Theory of Condensed Matter* (Springer-Verlag, Berlin, 1980), pp. 13–27.
[13] M. Huang, P. Zhuang, and W. Chao, Phys. Rev. D **67**, 065015 (2003); I. Shovkovy and M. Huang, Phys. Lett. B **564**, 205 (2003); M. Alford, C. Kouvaris, and K. Rajagopal, Phys. Rev. Lett. **92**, 222001 (2004).
[14] D. Ebert and K. G. Klimenko, J. Phys. G **32**, 599 (2006); L. He, M. Jin, and P. Zhuang, Phys. Rev. D **74**, 036005 (2006).
[15] Michael McNeil Forbes, E. Gubankova, W. V. Liu, and F. Wilczek, Phys. Rev. Lett. **94**, 017001 (2005).
[16] W. V. Liu and F. Wilczek, Phys. Rev. Lett. **90**, 047002 (2003).
[17] E. Taylor, A. Griffin, and Y. Ohashi, Phys. Rev. A **76**, 023614 (2007).
[18] H. Suhl, B. T. Matthias, and L. R. Walker, Phys. Rev. Lett. **3**, 552 (1959).
[19] V. M. Loktev, R. M. Quick, and S. G. Sharapov, Phys. Rep. **349**, 1 (2001).
[20] M. Iavarone, G. Karapetrov, A. E. Koshelev, W. K. Kwok, G. W. Crabtree, D. G. Hinks, W. N. Kang, E.-M. Choi, H. J. Kim, H. J. Kim, and S. I. Lee, Phys. Rev. Lett. **89**, 187002 (2002); F. Bouquet, Y. Wang, I. Sheikin, T. Plackowski, A. Junod, S. Lee, and S. Tajima, *ibid.* **89**, 257001 (2002); S. Tsuda, T. Yokoya, Y. Takano, H. Kito, A. Matsushita, F. Yin, J. Itoh, H. Harima, and S. Shin, *ibid.* **91**, 127001 (2003); J. Geerk, R. Schneider, G. Linker, A. G. Zaitsev, R. Heid, K. P. Bohnen, and H. v. Lohneysen, *ibid.* **94**, 227005 (2005).
[21] M. Köhl, H. Moritz, T. Stöferle, K. Günter, and T. Esslinger, Phys. Rev. Lett. **94**, 080403 (2005); L. M. Duan, *ibid.* **95**, 243202 (2005).
[22] M. Iskin and C. A. R. Sá de Melo, Phys. Rev. B **72**, 024512 (2005); Phys. Rev. B **74**, 144517 (2006).
[23] J.-P. Martikainen, E. Lundh, and T. Paananen, Phys. Rev. A **78**, 023607 (2008).
[24] A. I. Akhiezer, A. A. Isayev, S. V. Peletminsky, and A. A. Yatsenko, Phys. Lett. B **451**, 430 (1999).
[25] D. E. Sheehy and L. Radzihovsky, Phys. Rev. B **75**, 136501 (2007).
[26] R. Casalbuoni and G. Nardulli, Rev. Mod. Phys. **76**, 263 (2004).
[27] S. Takada and T. Izuyama, Prog. Theor. Phys. **41**, 635 (1969).
[28] L. He, M. Jin, and P. Zhuang, Phys. Rev. B **73**, 024511 (2006).